Improving sonar array performances with environment-informed sub-array processing

Alexandre L'Her[1,2], Angélique Drémeau[2], Florent Le Courtois[3], Gaultier Real[3], Xavier Cristol[1], and Yann Stéphan[4]

[1]Thales DMS, Valbonne, France
[2]Lab-STICC (UMR CNRS 6285), ENSTA Bretagne, Brest, France
[3]DGA Naval Systems, Toulon, France
[4]SHOM, Brest, France

alexandre.lher@ensta-bretagne.org

Abstract: *The wide range of environmental fluctuations present in underwater acoustic propagation affects sonar performance. In particular, internal waves can cause sonar arrays to lose signal coherence, reducing their gain. One of the most direct ways to mitigate this effect is to use sub-array processing. By taking the coherence radius (the average distance at which the signal received by two sensors can be assumed to be coherent) as the parameter determining the length of a typical sub-array, this method allows for more conventional processing methods to be used while assuming a coherent field on each sub-array. In this work, we use the Canonical Correlation Analysis (CCA) method to learn a model between acoustic and oceanographic variables, that is used to infer the coherence of the signal from environmental measurements at a latter time. To compensate for the loss of angular resolution, we introduce the use of a bayesian algorithm on the sub-arrays. We show on experimental data from the ALMA 2017 campaign that sub-array processing with a bayesian algorithm can improve detection performances when the coherence of the signal is degraded.*

Keywords: *Sub-array processing, canonical correlation analysis, sparse representations, SoBaP*

1. INTRODUCTION

Environmental fluctuations in underwater acoustics can be detrimental to sonar array performance. Ocean fluctuations, such as internal waves, will cause local variations of the sound celerity. This leads to a decrease in the spatial coherence of the acoustic wavefronts. Coherence of the acoustic pressure on the array is directly related to the array gain [Carey, 1998, Real et al., 2015], and sonar detection performance will be related to the ability to predict the acoustic coherence on the array. Several methods have been proposed to mitigate the effect of coherence loss on an array [Beaumont et al., 2018, Morgan and Smith, 1990, Lefort et al., 2017], but they rely on a previous knowledge or estimation of the coherence.

Oceanic fluctuations are very complex to describe. Therefore we will rely on statistical models to describe to infer acoustic fluctuations from some oceanographic measurements. In [L'Her et al., 2022], we showed that Canonical Correlation Analysis (CCA) can be used to find physical relationships between oceanographic and acoustic measurements, this motivates the use of CCA for the extraction of relationships to inform processing algorithms. The chosen algorithm is a sub-array processing scheme from the literature ([Cox, 1973, Lefort et al., 2017]), based on defining sub-arrays from the coherence length, *ie.* the mean length at which two sensors from the array remain correlated.

We will first present the ALMA 2017 campaign and the in-situ data. We will then present the sub-array method, and we will introduce the use of a Bayesian model from the literature to perform DOA estimation on the sub-arrays. We then explain the theory of CCA and introduce a generative version of the model. The generative model will be used, after prior training, to infer the acoustic coherence length from oceanographic variables only. Finally we present preliminary results of detection performance calculations of four studied DOA algorithms.

2. THE ALMA 2017 CAMPAIGN

ALMA (Acoustic Laboratory for Marine Applications) is a series of oceano-acoustic at-sea campaigns designed and operated by DGA Naval Systems [Real and Fattaccioli, 2018]. The 2017 campaign took place in the Western part of the Corsica Cape, in the Gulf of Saint Florent (Fig. 1 (left)). It included simultaneous oceanographic and acoustic measurements, with the goal of studying the effect of ocean fluctuations induced by internal waves on acoustic propagation.

The acoustic setup consists of two omnidirectional sources, and 4 32-element vertical linear arrays (VLA) 16.5 km away from the source. The array is spatially sampled at 5 kHz, which means that the hydrophones are separated by 15 cm. The deepest hydrophone of the array is at 110 m depth, where the total water depth is 140 m. The recordings are sampled at 48 kHz. In this work, we will use emissions from one source only, placed at 170m depth, and the measurements from one VLA of 32 elements. Figure 1 (right) shows a ray trace for the source at 170m depth in a range-independent celerity field constructed from an ARGO float profile taken at the date of the campaign. It shows the complexity of the acoustic field across the double canyon, with reflected and refracted rays.

The oceanographic setup consisted of a 150 m length, 24 elements thermistor chain. It sampled the temperature every 3 seconds, and was placed approximately 2 km away from the array. In Fig. 2 (left) we show the temperature measured by the thermistor chain during the campaign. We see many scales of fluctuations induced by internal waves : there are small oscillations on

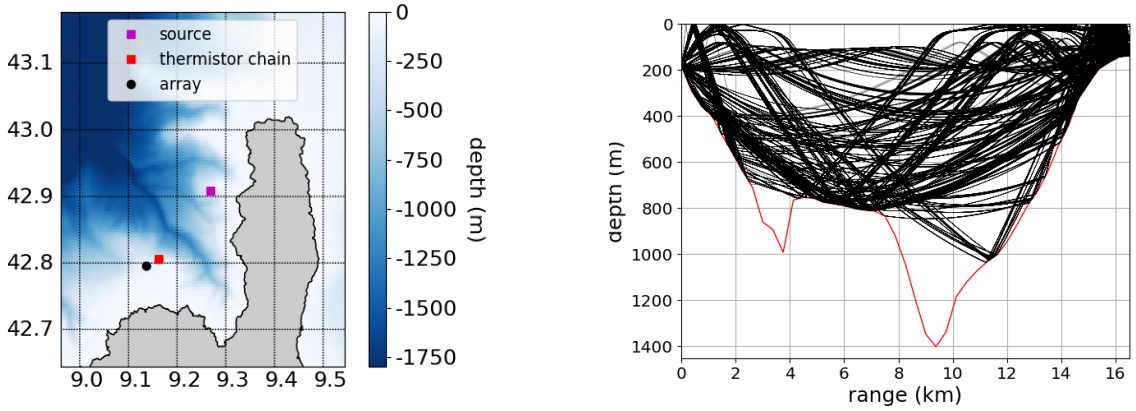

Figure 1: (left) ALMA 2017 location with its bathymetry and the positions of the source, thermistor chain and array. (right) Ray trace for the source at 170m depth in a range-independent case.

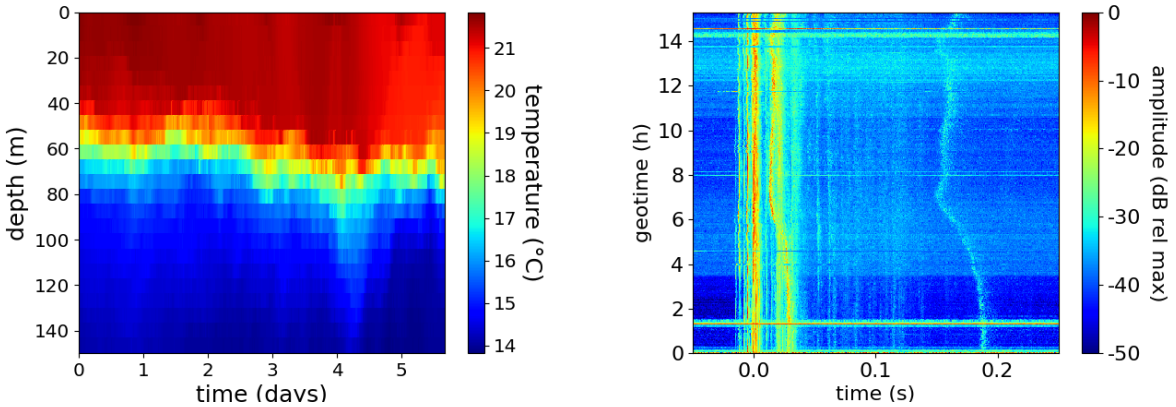

Figure 2: (left) Temperature measurements as a function of depth and time. (right) Impulse response of the 170m deep source, during a 15 h measurement phase.

the timescales of hours that will primarily interest us, and larger oscillations on scales of days that will not be studied in this work.

The acoustic emission sequences are notably composed of a linear frequency modulation (LFM) from 1 to 13 kHz during 10 s and 2 s long continuous waves (CW) at different frequencies (2,5,7,9,13) kHz. Each emission sequence duration is 1 min 30, alternating the source, *ie.* each source emits a sequence every 3 min. In Fig. 2 (right), we show the impulse response of the source at 170m depth during the longest acquisition phase, calculated using the LFM. There appear to be important smooth variations in the arrival-time of the last energetic arrival (between 0.15s and 0.2s), that seem to follow the fluctuations of the second strong arrival group (at around 0.02 s). We can also see smaller scale fluctuations with rays appearing or disappearing, or showing important amplitude variations from one ping to the next.

Overall, this shows the complexity of the time evolution of both the environment and acoustic propagation. The environmental fluctuations, on top of the complex acoustic propagation and a sparse knowledge of the environment makes it a very interesting campaign to study the relationships between environment knowledge and acoustic propagation.

3. SUB-ARRAY PROCESSING

To compensate for the loss of coherence, we consider the sub-array processing method published in [Lefort et al., 2017]. This method treats the beamforming problem as a convolution between the signal on the array and a window of the size of the coherence length. As a starting hypothesis, the effect of ocean fluctuations on the acoustic field is assumed to be modeled by a complex multiplicative noise as discussed in [Dashen et al., 2010, Ch. 8]. The pressure field received on the VLA of M sensors at time t is written in the frequency domain as :

$$\mathbf{y}_t = \mathbf{P}_t \mathbf{D} \mathbf{x}_t + \mathbf{n}_t, \tag{1}$$

where $\mathbf{P}_t$ is a diagonal matrix containing the multiplicative noises attached to the M sensors, $\mathbf{D}$ is a dictionary of N DOA (*i.e.* the i-th column of $\mathbf{D}$ is $\mathbf{d}(\theta_i) = [1, e^{j\frac{2\pi}{\lambda}\Delta\sin(\theta_i)}, \ldots, e^{j\frac{2\pi}{\lambda}(M-1)\Delta\sin(\theta_i)}]^T$, with $.^T$ the transpose operator, Δ the distance between two consecutive sensors and λ the wavelength of interest), $\mathbf{x}_t$ contains the contribution of the sources in each DOA in the dictionary and $\mathbf{n}_t$ is a complex Gaussian additive noise.

The method is detailed in [Lefort et al., 2017], it consists in extracting K arrays of the same length as the antenna, and weighting them by a sliding gaussian window. Then, for sub-array k, the new signal $\tilde{\mathbf{y}}_{k,t}$ is such that the multiplicative complex noise $\mathbf{P}_{k,t}$ can be assumed constant. We then fall back on a classical generative model in DOA estimation:

$$\tilde{\mathbf{y}}_{k,t} = \tilde{\mathbf{D}}_{k,t} \tilde{\mathbf{x}}_{k,t} + \tilde{\mathbf{n}}_{k,t}, \tag{2}$$

where $\tilde{\mathbf{D}}_{k,t} = \mathbf{W}_{k,t}\mathbf{D}$, $\tilde{\mathbf{n}}_{k,t} = \mathbf{W}_{k,t}\mathbf{n_t}$, $\tilde{\mathbf{x}}_{k,t} = \alpha_k \mathbf{x}_t$ with α_k the multiplicative noise, constant on the k-th sub-array. As in [Lefort et al., 2017], the weights of each sensor can be defined according to the mutual coherence function (MCF). In [Dashen et al., 1985], a theoretical model for the MCF is proposed as $\Gamma_t(m) = \exp(-\frac{m^2}{2L_c(t)^2})$, where m is the distance expressed in number of sensors between two sensors in the VLA and $L_c \in \mathrm{R}^+$ is called the "coherence radius" and approximates the relative space where two sensors remain correlated. Here sub-index t indicates that the MCF will vary as a function of time. As a consequence, the weights of the sensors can be defined by the MCF as $w_{k,t}(m) = \Gamma_t(|k-m|)$. This way, the sub-arrays will consist on average of coherent sensors, and eq. (2) will be valid. Finally, the outputs from the sub-arrays are incoherently summed to get the power spectrum at each time t and for each DOA i:

$$S_t(\theta_i) = \Big(\sum_{k=1}^{K} |\hat{x}_{k,t}(\theta_i)| \Big)^2. \tag{3}$$

Considering model (2), the DOA estimation can then be performed by solving an inverse problem. The most classical and popular method is beamforming, which focuses on the following problem : $\forall i \in \{1, \ldots, N\}$,

$$\hat{x}^{\mathsf{BF}}_{k,t}(\theta_i) = \mathsf{argmin}_{\tilde{x}_{k,t}(\theta_i)} \|\tilde{\mathbf{y}}_{k,t} - \tilde{\mathbf{d}}_{k,t}(\theta_i)\tilde{x}_{k,t}(\theta_i)\|_2^2 \tag{4}$$

where $\|.\|_2$ is the ℓ_2-norm, $\tilde{\mathbf{d}}_{k,t}(\theta_i)$ the i-th column in $\tilde{\mathbf{D}}_{k,t}$ and $\tilde{x}_{k,t}(\theta_i)$ the i-th element in $\tilde{\mathbf{x}}_{k,t}$.

As the use of sub-arrays reduces the angular resolution of the array, we applied a regularisation to the DOA estimation to regain the lost resolution. To solve such problems, methods exploiting a sparse model have recently come to the fore. These methods consider the regularised optimisation problem:

$$\hat{\mathbf{x}}^{\mathsf{SP}}_{k,t} = \mathsf{argmin}_{\tilde{\mathbf{x}}_{k,t}} \|\tilde{\mathbf{y}}_{k,t} - \tilde{\mathbf{D}}_{k,t}\tilde{\mathbf{x}}_{k,t}\|_2^2 + \mu\|\tilde{\mathbf{x}}_{k,t}\|_0, \tag{5}$$

where $\|.\|_0$ denotes the ℓ_0 pseudo-norm, counting the number of non-zero coefficients and μ is a Lagrangian multiplier. Problem 5 is NP-hard. Many sub-optimal algorithms have been proposed in the literature to solve it. Here, we propose to resort to the Bayesian algorithm SoBaP proposed in [Drémeau et al., 2012] and already considered in underwater acoustics in [Drémeau et al., 2017]. Note that both problems 4 and 5 rely on different assumptions on $\tilde{\mathbf{x}}_{k,t}$: Eq. 4 expresses a maximum likelihood estimation, while Eq. 5 considers a sparse model, by means of a Bernoulli-Gaussian model.

4. CANONICAL CORRELATION ANALYSIS

To define the length of the sub-arrays, it would be best to have a previous knowledge of the coherence length. Considering the influence of the medium on acoustic coherence, we aim to find relationships between acoustic variables and ocean measurements. As it can be complex to relate acoustic and oceanographic measurements, in particular when the knowledge of the environment is very limited, statistical methods are well suited to do it. Here we show the use of CCA. It is a method first published in [Hotelling, 1936], to relate two groups of variables. In a nutshell, it finds linear combinations of each group of variables, such that their correlation is maximum. In our case, those groups are composed of acoustic variables on one side and oceanographic variables on the other.

In [L'Her et al., 2022], we explicit the CCA model and show how this method can find physically-meaningful relationships between acoustic and oceanographic variables from *in-situ* data, in a shallow water range-independent context. We refer the reader to this article for theoretical development. CCA can also be reframed in the form of a generative predictor model. Let $\mathbf{A}$ be the matrix of the acoustic variables, and $\mathbf{B}$ the matrix containing the environmental variables. We then propose a two-step procedure : *i)* a training phase where $\hat{\Sigma}_{\mathbf{A}}$ and $\hat{\Sigma}_{\mathbf{B}}$, the canonical coefficient matrices, are estimated by the CCA method on the basis of both measurements training datasets $\mathbf{A}_{train}$ and $\mathbf{B}_{train}$. *ii)* The inference of $\hat{\mathbf{A}}_{test}$ from the canonical coeficient matrices and the environmental dataset $\mathbf{B}_{test}$:

$$\hat{\mathbf{A}} = \Lambda \mathbf{B}^T (\hat{\Sigma}_{\mathbf{B}}^T)^+ \hat{\Sigma}_{\mathbf{A}}^+, \tag{6}$$

where Λ is a diagonal matrix containing the canonical correlations. Using eq. (6), we can then infer acoustic variables from environmental measurements and the previously learned CCA model.

5. APPLICATION TO THE ALMA2017 CAMPAIGN

From the CW signals, the Mutual Coherence Function (MCF) was calculated, from which was extracted the mean array acoustic intensity and the coherence radius L_c as a function of time. Those are our acoustic variables for CCA. Empirical Orthogonal Functions (EOF) were calculated from the temperature data and from its vertical gradient. This allowed us to extract the temporal evolution of the spatial modes. Determining with Rule-N the number of EOF modes that we are allowed to consider, we took 3 modes of temperature and 2 modes of its vertical gradient. The time-evolution of those modes constitute the oceanographic group for CCA.

A running mean over 30 ping (equivalent to 1.5 hours) was applied to both datasets. This

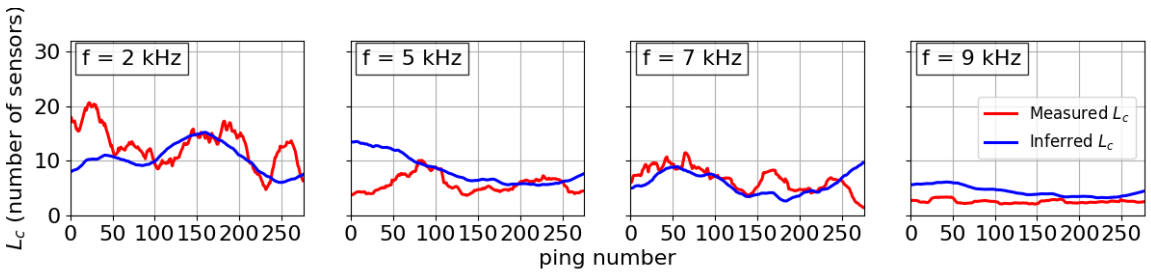

Figure 3: Measured (red) and inferred (blue) L_c from CCA, for the four studied frequencies.

running mean is necessary as the acoustic variables should be statistical quantities, but it also reduces the small temperature fluctuations that can be detrimental to CCA. The variables are also centered and reduced to unit variance, as required in the CCA framework. Learning the model from eq. (6), we can then estimate the reduced and centered L_c on the test phase from the temperature measurements. This estimation is rescaled by multiplying the standard deviation and adding the mean of L_c from the learning phase. We show the results in Fig. 3. The fits are not exact but we still capture some of the temporal variations. One problem occurs in particular when the mean and variance of L_c are drastically different between learning and test phase, in this case the re-scaling by the learning phase introduces an error. With the L_c approximated, we can now inform the sub-array processing as presented previously. Our scheme is particularly adapted to the problem of source detection. Indeed, L_c can be easily computed if we know that a desired signal is received. However, if we are unsure that a signal is present, having a prior estimation of its coherence can be beneficial.

We will use four algorithms on the data to compare their detection performances as a function of the mean L_c of the test phase : classical beamforming on the full array (FA CB), SoBaP on the full array (FA SB), classical beamforming on the sub-arrays (SA CB), SoBaP on the sub-arrays (SA SB). As we study in-situ data with a high SNR, we degraded the recordings by adding noise sampled from the corresponding pings (*ie.* we degrade the signal while preserving the temporal dependence of the noise). This allowed us to control the SNR values to study detection performances. Hereafter we show results for a SNR of 0 dB. The algorithms were run both on signal+noise and only noise to calculate respectively the probabilities of detection (P_d) and the probabilities of false alarm (P_{fa}) for various detection thresholds. They were used to trace the ROC curves and calculate their integrals up to $P_{fa} = 0.1$. A higher value means better capability to detect a source above the noise. As an additional metric, we can calculate the mean of $\frac{dP_d}{dP_{fa}}$ up to $P_{fa} = 0.1$. A higher value means that a small increase in false alarm probability gives a higher detection probability, and this is linked to better performances.

The integral of the ROC curves in Fig. 4 (left) shows that when the coherence of the wavefront is low, SoBaP with sub-arrays shows on average the highest detection performances. Additionally, SA CB is marginally better or equal to FA CB. It confirms that the sub-array algorithm is effective at compensating the coherence loss, as it had been shown in [Lefort et al., 2017] on simulated data. This behaviour is also seen on the derivative of the ROC curve, Fig. 4 (right). When L_c is low, the mean derivative is the highest when using SoBaP on sub-arrays. From both figures it also seems that CB on the full array or on sub-arrays does not change behaviour drastically with the coherence radius. When the coherence radius increases, SoBaP on the full array performs better. This is expected as the algorithm assumes a totally coherent array. We then get various ranges in L_c where different algorithms seem to be the best suited to maximize array detection performances. This result is adapted to our study case of the ALMA 2017 campaign,

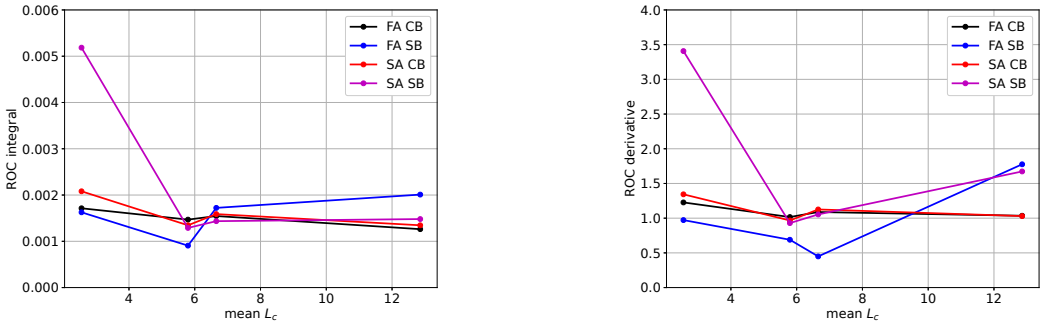

Figure 4: Integral (left) and derivative (right) of the ROC curves for a maximum false alarm propability of 0.1 as a function of the mean coherence radius, at 0 dB SNR.

and thus should be confirmed on other data.

6. CONCLUSION

Based on our previous work, we have used CCA to generate a linear model linking oceanographic and acoustic statistical data from a training phase. This model can later be used as a predictor of acoustic variables on an array (coherence length, mean-array intensity) using only temperature data.

In a second phase, the coherence length prediction helps to inform a sub-array processing algorithm and improve its performance in terms of ROC curves. First, the performance of classical beamforming was used and analysed on the full array and on sub-arrays. Shorter sub-arrays significantly reduce the angular resolution. Therefore, we attempted a regularisation scheme using SoBaP, a Bayesian algorithm from the literature, to recover the lost angular resolution. We show that SoBaP on sub-arrays increases the detection performances on experimental data when the coherence radius is small. On the contrary, when the coherence radius is larger, algorithms on the full array slightly outperforms sub-array methods.

It should be noted that the noise model assumed by SoBaP is Gaussian uniform. However, real noise is directional and does not always follow a Gaussian distribution. Some preliminary work on this issue using continuous DOA models is currently underway. This work could be a first step in an ocean-acoustic meta-modeling scheme that would combine pre-trained ocean acoustic models with in-situ oceanographic observations.

7. ACKNOWLEDGEMENTS

The authors thank Thales DMS and the French Defence Research Agency (AID) for funding.

REFERENCES

[Beaumont et al., 2018] Beaumont, G., Fablet, R., and Drémeau, A. (2018). An Approximate Message Passing Approach for DOA Estimation in Phase Noisy Environments. In Deville,

Y., Gannot, S., Mason, R., Plumbley, M. D., and Ward, D., editors, Latent Variable Analysis and Signal Separation, Lecture Notes in Computer Science, pages 385–394, Cham. Springer International Publishing.

[Carey, 1998] Carey, W. M. (1998). The determination of signal coherence length based on signal coherence and gain measurements in deep and shallow water. The Journal of the Acoustical Society of America, 104(2):831–837. Publisher: Acoustical Society of America.

[Cox, 1973] Cox, H. (1973). Line array performance when the signal coherence is spatially dependent. The Journal of the Acoustical Society of America, 54(6):1743–1746.

[Dashen et al., 1985] Dashen, R., Flatté, S. M., and Reynolds, S. A. (1985). Path-integral treatment of acoustic mutual coherence functions for rays in a sound channel. The Journal of the Acoustical Society of America, 77(5):1716–1722.

[Dashen et al., 2010] Dashen, R., Munk, W. H., Watson, K. M., and Zachariasen, F. (2010). Sound transmission through a fluctuating ocean. Cambridge University Press.

[Drémeau et al., 2012] Drémeau, A., Herzet, C., and Daudet, L. (2012). Boltzmann machine and mean-field approximation for structured sparse decompositions. IEEE Transactions on Signal Processing, 60(7):3425–3438.

[Drémeau et al., 2017] Drémeau, A., Le Courtois, F., and Bonnel, J. (2017). Reconstruction of dispersion curves in the frequency-wavenumber domain using compressed sensing on a random array. IEEE Journal of Oceanic Engineering, 42(4):914–922.

[Hotelling, 1936] Hotelling, H. (1936). Relations Between Two Sets of Variates. Biometrika, 28(3/4):321–377. Publisher: JSTOR.

[Lefort et al., 2017] Lefort, R., Emmetiere, R., Bourmani, S., Real, G., and Drémeau, A. (2017). Sub-antenna processing for coherence loss in underwater direction-of-arrival estimation. Journal of the Acoustical Society of America, 142(4):2143–2154. Publisher: Acoustical Society of America.

[L'Her et al., 2022] L'Her, A., Drémeau, A., Le Courtois, F., Real, G., Cristol, X., and Stéphan, Y. (2022). Canonical correlation analysis as a statistical method to relate underwater acoustic propagation and ocean fluctuations. JASA Express Letters, 2(10):100801. Publisher: Acoustical Society of America.

[Morgan and Smith, 1990] Morgan, D. R. and Smith, T. M. (1990). Coherence effects on the detection performance of quadratic array processors, with applications to large-array matched-field beamforming. The Journal of the Acoustical Society of America, 87(2):737–747. Publisher: Acoustical Society of America.

[Real et al., 2015] Real, G., Cristol, X., Habault, D., Sessarego, J., and Fattaccioli, D. (2015). Influence of de-coherence effects on sonar array gain : scaled experiment, simulations and simplified theory comparison. In UACE2015 3rd Underwater Acoustics Conference & Exhibition, Chania, Greece.

[Real and Fattaccioli, 2018] Real, G. and Fattaccioli, D. (2018). Acoustic laboratory for marine applications: Overview of the alma system and data analysis. OCEANS 2018 MTS/IEEE Charleston, pages 1–7.